Monopod bucket foundations under cyclic lateral loading

Foglia, Aligi; Ibsen, Lars Bo

Publication date:
2014

Document Version
Publisher's PDF, also known as Version of record

Monopod bucket foundations under cyclic lateral loading

Aligi Foglia
Lars Bo Ibsen

DEPARTMENT OF CIVIL ENGINEERING
AALBORG UNIVERSITY

ISSN 1901-7278
DCE Technical Memorandum No. 49

Aalborg University
Department of Civil Engineering
Division of Structures, Materials and Geotechnics

DCE Technical Memorandum No. 49

Monopod bucket foundations under cyclic lateral loading

by

Aligi Foglia
Lars Bo Ibsen

September 2014

Scientific Publications at the Department of Civil Engineering

Technical Reports are published for timely dissemination of research results and scientific work carried out at the Department of Civil Engineering (DCE) at Aalborg University. This medium allows publication of more detailed explanations and results than typically allowed in scientific journals.

Technical Memoranda are produced to enable the preliminary dissemination of scientific work by the personnel of the DCE where such release is deemed to be appropriate. Documents of this kind may be incomplete or temporary versions of papers—or part of continuing work. This should be kept in mind when references are given to publications of this kind.

Contract Reports are produced to report scientific work carried out under contract. Publications of this kind contain confidential matter and are reserved for the sponsors and the DCE. Therefore, Contract Reports are generally not available for public circulation.

Lecture Notes contain material produced by the lecturers at the DCE for educational purposes. This may be scientific notes, lecture books, example problems or manuals for laboratory work, or computer programs developed at the DCE.

Theses are monograms or collections of papers published to report the scientific work carried out at the DCE to obtain a degree as either PhD or Doctor of Technology. The thesis is publicly available after the defence of the degree.

Latest News is published to enable rapid communication of information about scientific work carried out at the DCE. This includes the status of research projects, developments in the laboratories, information about collaborative work and recent research results.

Published 2014 by
Aalborg University
Department of Civil Engineering
Sofiendalsvej 9-11,
DK-9200 Aalborg SV, Denmark

Printed in Aalborg at Aalborg University

ISSN 1901-7278
DCE Technical Memorandum No. 49

Monopod bucket foundations under cyclic lateral loading

Abstract

The monopod bucket foundation can be a cost-reducing sub-structure for offshore wind turbines. To avoid problems during the turbine operation, the long-term effect of cyclic loading must be considered in the design of the foundation. In this paper a 1*g* testing rig is adopted to extend the knowledge on bucket foundations under lateral cyclic loading. The test setup is described in detail and a comprehensive experimental campaign is presented. The foundation is subjected to cyclic overturning moment, cyclic horizontal loading and constant vertical loading, acting on the same plane for thousands of cycles. Three buckets with different embedment ratios are tested. The data interpretation is focused on the long-term permanent rotation of the foundation and, particularly, on understanding how the controlling variables influence the potential for rotation accumulation. New and more general parameters of an empirical model predicting the long-term plastic rotation are proposed on the base of the experimental results.

List of notation

γ'	effective unit weight of the sand
D_r	relative density of the sand
D	foundation diameter
d	foundation embedment (skirt length)
t	wall thickness
f_L	cyclic loading frequency
N	number of cycles
H	horizontal load acting on the load reference point
h	eccentricity of the horizontal load
M	overturning moment acting on the load reference point $M = hH$
M_R	ultimate monotonic moment
M_{max} , M_{min}	maximum and minimum cyclic overturning moment
H_{max} , H_{min}	maximum and minimum horizontal load
V	vertical load acting on the load reference point
θ_N	rotational displacement of the foundation after N cycles
θ_0	rotational displacement of the foundation at $N = 1$
θ_s	rotational displacement of the foundation under monotonic loading when $M = M_{max}$
θ_T	rotation tolerance
θ_f	rotational displacement at the end of a cyclic test
$\tilde{\theta}_N$	normalised accumulated rotation
ζ_b	cyclic loading magnitude ratio, $\zeta_b = M_{max} / M_R$
ζ_c	cyclic loading ratio, $\zeta_c = M_{min} / M_{max}$
T_b, T_c, α	parameters of the empirical model

1. Introduction

To make offshore wind competitive in the energy market, cost-effective solutions for foundations and installation technologies must be developed. The monopod bucket foundation, given the right soil profile, can be a cost-reducing sub-structure for offshore wind turbines. This steel structure includes a bucket foundation and a conical shaft. The shaft is the interface between the support structure and the turbine tower. As opposed to monopile foundations, no transition piece is needed. The bucket foundation, known also as suction caisson, is a shallow skirted foundation with circular cross section of diameter, D and skirt length, d. This foundation concept has been adopted for decades in the oil and gas industry as an alternative to drilling or driving for anchoring mooring buoys (Senpere and Auvergne, 1982) or as a foundation for jackets (Bye et al., 1995). A picture of a monopod bucket foundation placed on the deck of an installation vessel is shown in Figure 1. This full-scale structure was installed at Dogger Bank, in the British Sector of the North Sea. The dimensions of this structure are: D = 15 m, d = 7.5 m and wall thickness, t = 30 mm.

The installation consists of two phases: first, the foundation penetrates the seabed for a few meters by its own weight; second, suction assisted penetration is carried out until the skirt is fully embedded. This installation technology prevents the generation of noises that can be harmful for marine mammals. Furthermore, such installation process can be fully reversed, ensuring the full recovery of the structure at the end of the lifetime. DNV (2011) states that repeated loading may lead to irreversible soil deformation (and thus irreversible foundation displacement) that could jeopardize the turbine operation. When designing in the serviceability limit states (SLS) or in the fatigue limit states (FLS), this is to be accounted for by calculating the cumulative displacement with an adequate method.

Figure 1: Large-scale monopod bucket foundation on the deck of a jackup vessel

Another important consequence of repeated loading is that it may lead to changes in the natural frequency of the system and, in the worst case, trigger resonance.
The offshore environment presents adverse loading conditions, *i.e.* large overturning moment, M, and horizontal load, H, due to the action of waves. The condition is worsened for offshore wind turbines as these are light structures with $M/(VD)$ typically larger than 1.

The drained and undrained response of shallow embedded foundations under general loading is widely explored in literature (Gourvenec, 2007; Villalobos et al., 2009, Barari et al. 2012, Achmus et al. 2013b, Ibsen et al., 2014a, Ibsen et al., 2014b). Andersen (2009) presents a framework to estimate the settlements of shallow foundations subjected to cyclic loading due to storms. A well-established method to predict the response of offshore foundations under long-term cyclic lateral loading (*i.e.* millions of load cycles) does not exist yet. Lately, many research contributions have been given to this issue. Numerical models of monopiles were developed by Achmus et al. (2009) and subsequently by Depina et al. (2013). Monopiles were also tested in single gravity physical models by Peralta (2010) and Taşan et al. (2011). Centrifuge modelling has also been attempted. Watson and Randolph (2006) carried out an experimental campaign testing a bucket foundation and deriving fatigue contours for few hundreds of cycles. More recently Klinkvort and Hededal (2013), Garnier (2013) and Kirkwood and Haigh (2014) run lateral cyclic loading centrifuge tests on monopiles. Achmus et al. (2013a) run numerical simulations of bucket foundations under cyclic loading investigating the effect of load magnitude, relative density and embedment ratio, d/D.
Comprehensive state of the art studies on cyclic loading of offshore foundations are Jardine et al. (2012), Randolph (2012) and Andersen et al. (2013).

This paper deals with the issues related to permanent displacements of bucket foundations engendered by cyclic loading. In particular, the accumulation of rotational displacement is addressed, as recommended by standards (DNV, 2011) and industry practice. A similar study on this issue has been conducted by Zhu et al. (2013). They performed tests on dry loose sand with a bucket of D = 200 mm, and d/D = 0.5 under two different vertical loads. The experimental data was interpreted with the empirical model proposed in LeBlanc et al. (2010) and the parameters of the model were found independent of the vertical load applied.
The main objective of this study is to generalise the method to buckets with three different embedment ratios. A comprehensive experimental campaign concerning bucket foundations subjected to lateral cyclic loading is presented. The physical model design is thoroughly described and the experimental results are interpreted. The effect of loading frequency and relative density on the pattern of response is addressed. The post-cyclic behaviour and the robustness of the foundation in terms of cyclic loading are also investigated. In order to add practical value to the study, cyclic capacity curves are constructed and used in a design case.

2. Physical model design

2.1 Scope and aims of the modelling

Conducting geotechnical experiments in 1g is a delicate issue and, when designing the experimental setup, all the choices must be choices of meaning. The geotechnical system taken as prototype to resemble in

small-scale experiments is a bucket foundation supporting a 5 MW wind turbine installed in dense silica sand. The diameter of the foundation is D = 15 m while the moment to horizontal load ratio is $M/(HD)$ = 2. The scale of the model is 1:50.

In general, when the results of small-scale experiments are to be scaled up, adequate scaling laws are required. In this work, rather than scaling up results directly to prototype scale, the intention is to capture general behavioural patterns of the foundation. To recreate similar responses in two different scales, non-dimensional groups are to be retained between small-scale and prototype-scale. Three simple dimensionless groups were considered in this study: $M/(HD)$, t/D and $V/(\gamma' D^3)$ where γ' is the effective unit weight of the sand and V is the vertical loading. In real-scale wind turbine structures V includes the self-weight of the foundation and the weight of the whole superstructure. A realistic ratio $V/(\gamma' D^3)$ for large-scale bucket foundations supporting wind turbines ranges between 0.1 and 1. The typical value of t/D lies in the range 0.002 – 0.003. As these groups were to be conserved, the physical model was designed accordingly. For the entire experimental campaign $M/(HD)$ was set to 1.98 while $V/(\gamma' D^3)$ was between 0.73 and 0.89, depending on the bucket tested. The non-dimensional group t/D was 0.005 for all the buckets. Although the latter exceeds the maximum value suggested by industry practice, it is deemed that this group would affect the model accuracy only in case of differences in order of magnitude.

Since the pore pressure development is not of primary interest in this study, the loading frequency was not scaled and only tests conducted in substantially drained conditions were interpreted with the empirical model. The drainage condition of the tests was evaluated on the base of the findings of Foglia et al. (2013) as explained further in the paper.

It is well-known that realistic shear strength of the soil in 1*g* models can be achieved by increasing the void ratio of the soil we would have in large-scale. In so doing the path toward the critical state line of the soil in small-scale would resemble that in large-scale and dilation would be suppressed (Cerato and Lutenegger, 2007, LeBlanc et al., 2010, Wood, 2004). However, here the aim is not to scale up the ultimate capacity and the stiffness of the monotonic behaviour. If serviceability and fatigue limit state design situations are investigated, the load magnitudes involved are limited and no dilation is likely to occur. Thus, it is argued that preparing the sand at very low D_r would result in samples more prone to disturbance and, more importantly, would lead to overly conservative results in terms of permanent displacements as a result of an unrealistic potential for compaction. For this reason, in an attempt to better capture the displacements accumulation, the relative density of the prototype-scale is conserved in small-scale. The samples were densely packed also to obtain general failure of the foundation and gain thereby a clear reference failure moment from the monotonic tests.

The aim of this experimental campaign was to extend the previous analysis of Zhu et al. (2013) by changing some essential features of the model. The novel analysis concerns buckets of three different bucket geometries, the effect of loading frequency and the post-cyclic behaviour. Besides, the soil sample is water saturated, densely packed and the foundations tested are 100 mm larger in diameter.

2.2 Description of the model

The experimental rig used to carry out the testing program was designed and constructed at Aalborg

University. The system was designed on the base of the rig employed by LeBlanc et al. (2010). A sketch of the equipment is illustrated in Figure 2. A sand box (1600 x 1600 x 1150 mm) and a loading frame are the main components of the setup. The sand box is made of steel and is equipped with a drainage layer at the bottom. The drainage system consists of perforated pipes, 100 mm of drainage material (gravel) and sheets of geotextile dividing the layers. The pipes let the water evenly within the sand container. The water is provided by a tank and the water gradient is regulated with valves. The loading frame surrounds the sand box and provides a firm support to the equipment for monotonic and cyclic loading. Two screw jacks are mounted on the sides of the loading frame, one for lateral monotonic loading and the other for the foundation installation. To apply cyclic loading to the foundations, the rig is integrated with a loading beam hinged on one side of the box, four pulleys, three weight-hangers, few meters of steel wire and additional steel frame. An electric motor capable of exerting constant rotational motion is mounted on the hinged beam. The cyclic loading is induced to the system by applying a rotational motion to weight-hanger 1 which in turn cause the hinged beam to oscillate in the vertical direction.

The foundation is subjected to cyclic loading through a vertical beam bolted on the bucket lid which is directly connected to the system with two wires, one on each side. The features of the cyclic loading applied can be adjusted by changing the set of weights on the weight-hangers. Three foundations with diameter, D = 300 mm, and embedment ratios equals to 1, 0.75 and 0.5, were tested. Throughout the paper the buckets will be addressed by using their embedment ratio (d/D = 1, d/D = 0.75 and d/D = 0.5). The skirts of the foundations have all the same wall thickness, t = 1.5 mm. This particular thickness was chosen in order to ensure a fully rigid response of the foundations during any loading phase. The foundations are instrumented with three linear variable differential transformers (LVDTs). Two load cells are mounted on the vertical bar to record the net load applied to the foundation. A PC-based data acquisition system is used to transfer data from the measurement devices to the computer. The data sampling frequency is set to 2 Hz. The soil used for conducting the experimental program is Aalborg University Sand No. 1 (*cf.* Table 1 for properties). The reference system taken for forces and displacements is that proposed by Butterfield et al. (1997).

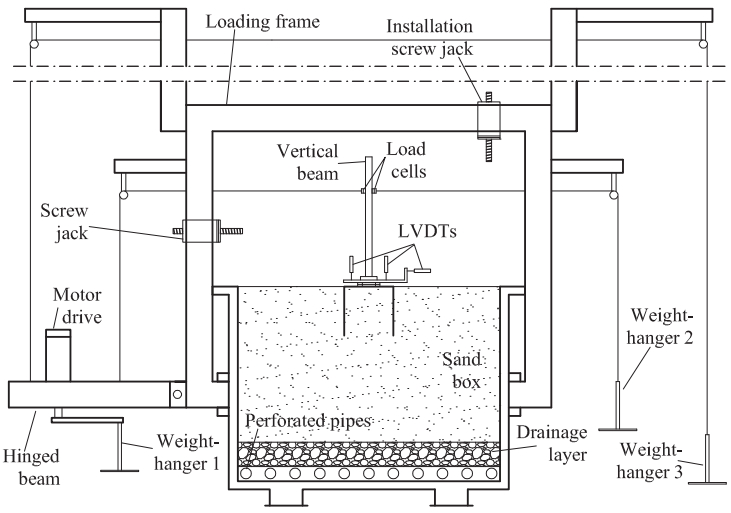

Figure 2: Schematic illustration of the testing rig

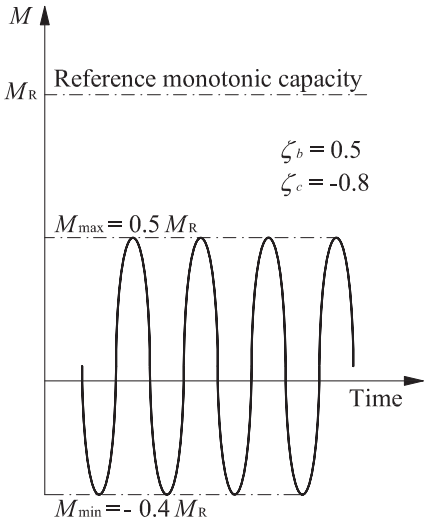

Figure 3: Example of biased two-way cyclic loading

Each cyclic test was carried out in four stages: sample preparation, installation, cyclic loading test and post-cyclic monotonic test. To ensure repeatability, a systematic sample preparation procedure was carried out before each test. A gradient close to the critical one was applied to the sample. Thereafter, mechanical vibration of the sand was performed. After vibrating, the uniformity and the compaction state of the sample were assessed by analysing small-scale cone penetration tests (CPT) performed in three different positions. The sample had a high compaction state, average D_r = 89 %. The bucket was installed in the middle of the sand box by means of a screw jack with a penetration rate of 0.02 mm/s. The foundation was installed by pushing rather than by applying suction. This has certainly an effect on the foundation capacity (Villalobos, 2006). However, the potential for rotational displacement accumulation should not be significantly affected as it is normalised with the monotonic reference rotation (see the next section).

Three air valves placed on the lid were let open during the penetration. Once the installation stage was complete, the installation rig was dismantled and the air valves were sealed to ensure full contact between soil and bottom lid during the test. The vertical beam was then bolted on the bucket lid and connected to the system. The number of cycles applied was between $1 \cdot 10^4$ and $5 \cdot 10^4$. At the end of the cyclic stage the cyclic equipment was meticulously substituted with the monotonic one to run the post-cyclic test. Cyclic loading tests were load-controlled. With respect to the load reference point the foundation was subjected to sinusoidal cyclic horizontal load, $H_{\min} \leq H \leq H_{\max}$, sinusoidal cyclic overturning moment, $M_{\min} \leq M \leq M_{\max}$, and constant vertical load, V (self-weight of the foundation and weight of the vertical beam).

The reference monotonic tests were controlled by designating a displacement rate to the point of load application. Foglia et al. (2013) conducted test of bucket foundations controlled in the same manner. The foundations were instrumented with eight pore pressure transducers placed under the lid and along the skirt. Four different displacement rates were tested. Tests carried out with displacement rate in the range 0.01 – 0.1 mm/s were found to be in substantially drained conditions. Based on this finding, the reference monotonic experiments were designed as displacement-controlled quasi-static tests with a displacement rate imposed by the actuator of 0.011 mm/s.

Table 1. Properties of Aalborg University Sand No. 1

Property	Value	Unit
Grain diameter corresponding to 50 % passing	0.14	[mm]
Uniformity coefficient	1.78	[-]
Specific grain density	2.64	[-]
Maximum dry unit weight	17.03	[kN/m^3]
Minimum dry unit weight	14.19	[kN/m^3]

2.3 Experimental program

Before describing all the phases of the experimental program, it is necessary to outline the key elements of the empirical model used to analyse the data (LeBlanc et al., 2010). The object of the empirical model is the relationship between the normalised accumulated rotation, $\tilde{\theta}_{\mathrm{N}}$, and the number of cycle N:

$$\tilde{\theta}_{\mathrm{N}} = \frac{\theta_{\mathrm{N}} - \theta_0}{\theta_{\mathrm{s}}} = T_b(\zeta_b, R_d) T_c(\zeta_c) N^{\alpha} \quad (1)$$

where θ_{N} is the accumulated rotation at cycle of number N, θ_0 is the rotation at the first cycle, θ_{s} is the rotation of the monotonic test at $M = M_{\max}$ and T_b, T_c and α are the parameters of the model. T_b and T_c depend on the cyclic loading features ζ_b and ζ_c which are defined as follows:

$$\zeta_b = \frac{M_{\max}}{M_{\min}}, \zeta_c = \frac{M_{\min}}{M_{\mathrm{R}}} \quad (2)$$

A graphical representation of the two ratios is given in Figure 3.

The model is defined by means of the boundary condition T_c (ζ_c = 0) = 1.

The experimental campaign comprises seven test series. Each of them was conducted with clear intention and with great attention to details. Table 2 (see at the end of the paper), lists all the tests of the experimental campaign.

In Series 1, 5 and 6, ζ_c was set to 0 and thereby the parameters T_b could be deduced for the three buckets. In Series 2, ζ_b was set to approximately 0.37 to obtain the parameter T_c. In Series 3 the robustness of the foundation against cyclic loading was addressed by conducting tests at increasing ζ_b. Series 4 was devoted to investigate the influence of the loading frequency on the cyclic behaviour. Series 0 includes the three monotonic reference tests.

Technical problems denied the post-cyclic stages of C47 and C39 to be performed.

3. Results

3.1 Presentation of typical results

Selected results are presented in order to give an insight into the general behavioural patterns of bucket foundations under lateral cyclic loading. It is common practice to present the results of small-scale experiments in non-dimensional form. However, in this section qualitative and scaling-independent results are shown. Thus, it was deliberately chosen to present the results without scaling.

Figure 4 shows how the rotational displacement accumulates for two tests and a magnified view of few cycles. Even though cyclic amplitude and mean value are very dissimilar in magnitude, the accumulation rate appears fairly comparable. In Figure 5, the three monotonic reference tests are plotted. Test S30 developed a clear general failure mechanism, with a noticeable peak in moment capacity followed by a softening branch. Tests S57 and S48, did not show a distinct peak in moment capacity. Instead, a plateau followed by a moderate negative gradient took place. Although the relative density is very high, the general failure of the system occurs only for the foundation with the largest embedment ratio. This kind of response could be seen in analogy with the findings of Vesić (1973), who investigated how the failure mechanism of shallow foundations under pure vertical loading changes as a function of D_r and d/D. M_{R} was taken as the maximum moment reached during the test. In the same graph, the points corresponding to the first cycle of all the cyclic tests of d/D = 1 are depicted. All the points, except for those of the two tests with highest moment (C39 and C40), lie along the monotonic curve. This proves the substantially drained condition of these tests. The two tests that deviate from the monotonic test had most likely too high loading rate to remain substantially

drained. Though, it should be emphasised that the tests which underwent partly drained conditions are not taken into consideration when interpreting the data with the empirical model.

It is worth to notice that also the tests conducted at different loading frequencies (squares on Figure 5) follow the fully drained response. Even further in the tests, no significant and consistent alteration of the behaviour in terms of displacements was found between the tests of Series 4.

In Figure 6, the rate of displacement accumulation in terms of rotation (*i.e.* the permanent rotation accumulated every ten cycles, θ_{N+10} - θ_N) is plotted against N for three tests of series 2. In general, when the rate of accumulation grows with the number of cycles, cyclic progressive failure occurs. This is not the case for the tests shown in Figure 6. The plot shows a significant rotational displacement accumulation within the first hundreds of cycles, followed by a plastic adaptation in which the rate of accumulation gradually decreases until reaching a negligible value. As expected, the larger the ζ_b the more number of cycles are required for the accumulation rate to reduce.

In Figure 7, the ultimate post-cyclic moment against the rotation at failure of all the tests of d/D = 1 is plotted. The large majority of the points exceeds the reference moment (test S30). On average, the post-cyclic capacity is 10.5 % larger than the reference capacity.

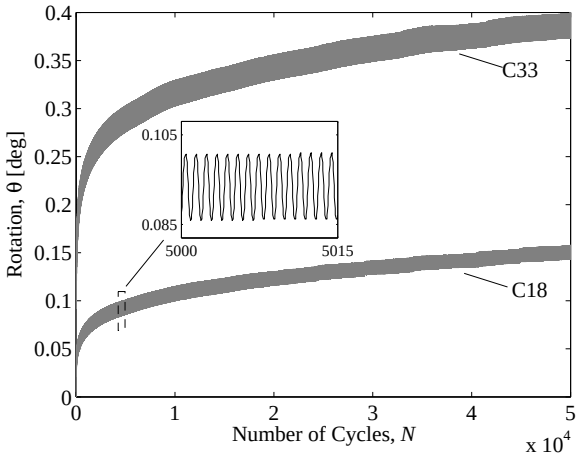

Figure 4: Rotational displacement accumulation for two different tests and magnified view of few cycles

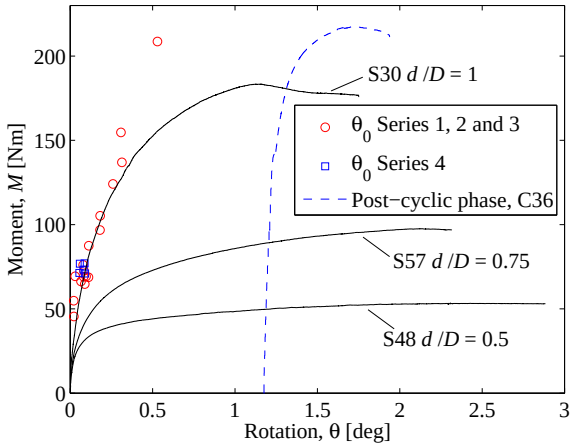

Figure 5: Reference monotonic tests S30, S48 and S57, post-cyclic phase of C36 and points relative to the maximum rotation of the first cycle

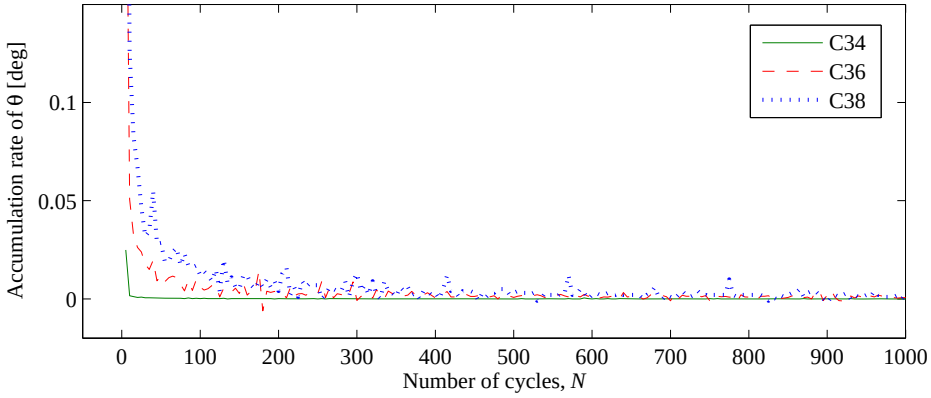

Figure 6: Accumulation rate of the rotational displacement of tests C34, C36 and C38 for the first 1000 cycles

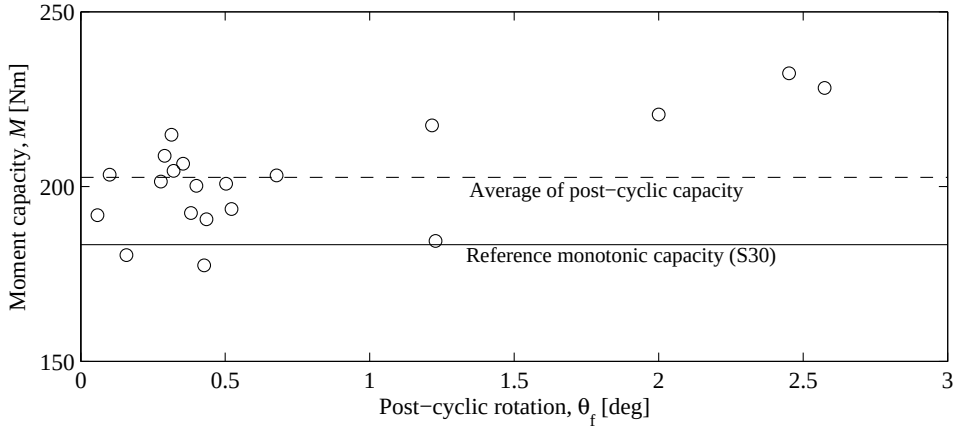

Figure 7: Post-cyclic moment capacity for series 1, 2 ,3 and 4 compared to the monotonic capacity

The same observation can be made in Figure 5 on the *M*-θplane where the post-cyclic phase of test C36 is plotted. The post-cyclic curve has higher initial stiffness and capacity than the reference monotonic curve. The failure mechanism is brittle as for the monotonic test.

3.2 Interpretation of the results

Equation 1 is used to fit all the tests run in substantially drained conditions. In general, the exponent α has the tendency to reduce as *T* increases. This suggests that when a foundation system accumulated significant rotational displacement in the beginning, it has less potential for accumulation further in the test. This is in accordance to what pointed out by Achmus et al. (2013a) where the ratio θ_N/θ_0 was found to have a higher rate for low values of ζ_b. A clear dependency of α on the test features could not be detected and, therefore, a constant exponent was used to analyse the data. When fitting all the drained tests until *N* = 10000 with Eq. (1), the average α turns out to be 0.189 with a standard deviation of 0.034. The value of α differs significantly from that of Zhu et al. (2013) and this is to be ascribed to the different relative density of the sands.

The results of series 1, 5 and 6 are presented in Figure 8. The points extrapolated using three different bucket geometries seem to follow the same trend. This indicates that the parameter T_b does not depend on the embedment ratio. This observation contrasts with Achmus et al. (2013b) who found the accumulated rotation to be slightly higher for *d*/*D* = 0.5. An interpolating curve in the form of a power law was chosen to fit the data:

$$T_b = 2.41\zeta_b^{1.64} \tag{3}$$

In Figure 8, the fit proposed by Zhu et al. (2013) is also plotted. The discrepancy between the two trends proves the T_b-dependency on the relative density. The same pattern (*i.e.* T_b reducing for looser compaction states) was found by LeBlanc et al. (2010). Recently, T_b was found dependent on the particle size in a study conducted by Abadie and Byrne (2014). However, the uncoupled effect of these two properties of the system has not been identified yet. The experimental points of series 2, together with the fit deduced by Zhu et al. (2013), are shown in Figure 9.

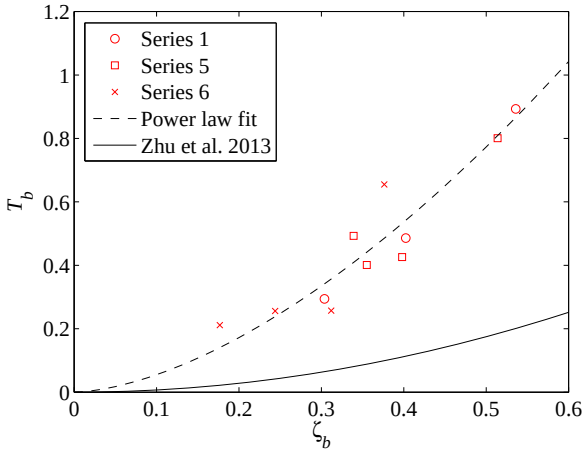

Figure 8: T_b parameter: Zhu et al., 2013, experimental points of this work and relative fit

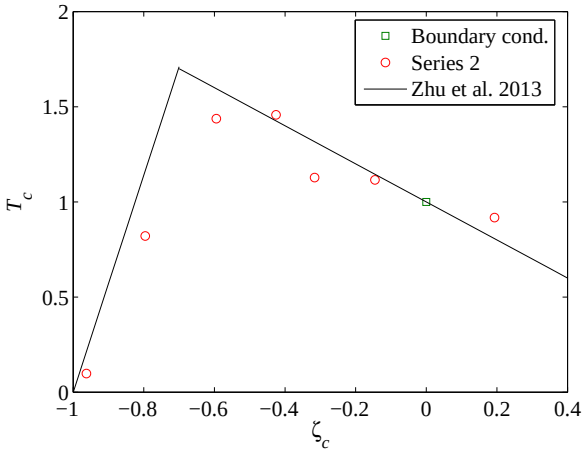

Figure 9: T_c parameter: Zhu et al., 2013 and experimental points of this work

Despite the significantly different embedment ratio and relative density, the experimental points match the fit. It can be concluded that T_c depends neither on the embedment ratio, nor on the relative density. The tests of Series 2 also support the idea that T_c peaks in correspondence to a biased two-way loading configuration. Interestingly, Kirkwood and Haigh (2014) attributed this phenomenon to the reduction of locked in stresses occurring in presence of biased two-way loading conditions.

4. Implication to foundation design

From the observations on the post-cyclic behaviour (Figure 5 and Figure 7) two distinct implications emerge. Firstly, since the foundation was pre-subjected to cyclic M and H the yielding surface expanded and therefore it is not surprising that the initial stiffness increases. Secondly, and perhaps more importantly, the failure envelope seems to increase when a foundation is pre-subjected to cyclic loading.

In the following, an example of how to put into practice the empirical model is given. As explained earlier in the paper, no direct result of the tests is scaled up by means of scaling laws. Instead, it is assumed that when the dimensionless groups of large-scale systems are similar to those used in the experimental campaign, the general relationship found in small-scale between monotonic and cyclic response is applicable in large-scale.

The example consists in a preliminary estimation of the long-term accumulated rotation of a bucket foundation supporting a 5 MW wind turbine. The estimation is preliminary in the sense that it is based only on the empirical model which would need to be validated against real-scale measurements over many years of turbine operation. As substantially drained conditions are considered, it is reasonable to assume $\theta_0 = \theta_s$.

The features of the bucket foundation are D = 15 m, d/D = 0.75 and t = 30 mm. The foundation is subjected to general loading: constant vertical loading, V = 35 MN, cyclic overturning moment and cyclic horizontal loading. A one-way loading configuration (ζ_c = 0) is chosen and the analysis evaluates both SLS and FLS design cases. According to LeBlanc et al. (2010), typical design cases for offshore wind turbines are for SLS, $N = 10^2$ and $\zeta_b = 0.473$, whereas for FLS, $N = 10^7$ and $\zeta_b = 0.295$.

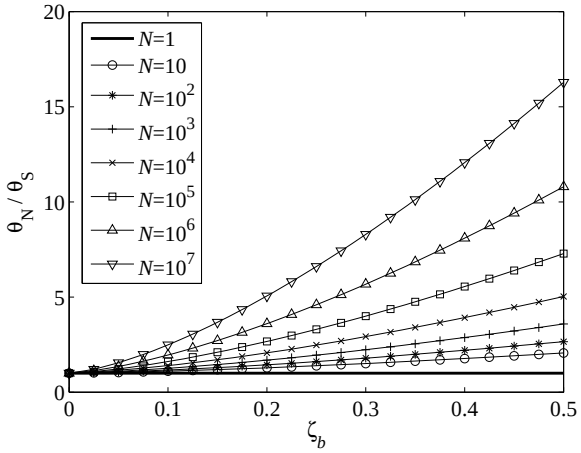

Figure 10: Normalised accumulated rotation as a function of the number of cycles and ζ_b

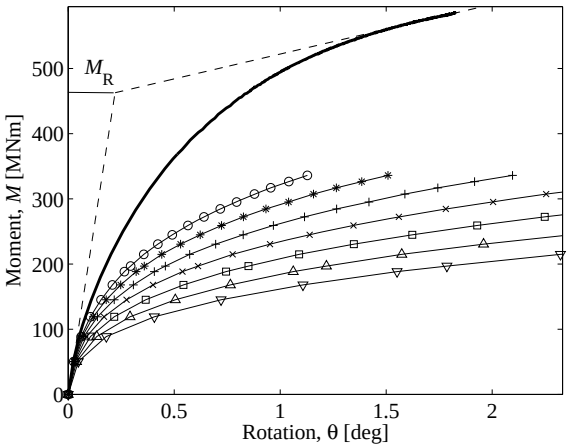

Figure 11: Cyclic capacity curves as opposed to monotonic capacity curves

By simply combining Equations 1 and 3 the accumulated rotation as a function of loading configuration and number of cycle can be evaluated:

$$\frac{\theta_N}{\theta_s} = 1 + \left(2.41\zeta_b^{1.64}\right) I_c N^{0.189} \tag{4}$$

A design graph relevant to the loading case in object, and based on Equation 4, is illustrated in Figure 10. To use Figure 10 in the design case, it is necessary to evaluate the monotonic $M - \theta$ curve in some manner. For this purpose, a drained numerical simulation is performed with the software Plaxis 3D. The Hardening Soil Model is used to run the drained simulation. Typical dense silica sand parameters are adopted. The ultimate moment capacity is defined by the intersection between the tangents to the initial and final points of the curve (M_R = 462.74 MNm). Equation 4 can be used to estimate the accumulated displacements for SLS design, $\theta_{N,\ SLS}$ = 0.506, and FLS design $\theta_{N,\ FLS}$ = 0.749. Some authors adopt a very stringent 0.5º as maximum rotation criterion justifying such a choice as the limit recommended by DNV (2011). However, DNV (2011) suggests this value in the context of a mere example and, in some cases, this stringent limit might lead to over-conservative design. The rotation tolerance relative to the normal operation of the wind turbine should instead be defined by the turbine manufacturer and the contractors on a case by case basis.

In order to have a graphical understanding of the secant stiffness degradation due to repeated loading, cyclic capacity curves can be constructed on the base of Equation 4 and the monotonic M-θ curve. This can be accomplished by simply calculating θ_N for different values of N and ζ_b. The cyclic capacity curves are plotted in Figure 11 as opposed to the monotonic curve. The legend of Figure 10 applies also to Figure 11. By entering the graph with the appropriate N and ζ_b, $\theta_{N,\ SLS}$ and $\theta_{N,\ FLS}$ can be graphically found.

5. Limitations of the physical model

The lateral cyclic loading is applied in terms of sinusoidal and continuous M and H.

In reality, environmental loads do not fluctuate regularly about a mean value. Imposing sinusoidal M

and *H* on the foundation is, in fact, unrealistic and leads inevitably to conservative prediction of displacements (Byrne, 2000). If realistic displacements are to be predicted, a relationship between real wave load patterns and equivalent sinusoidal load should be established.

Offshore environment is featured by a combination of waves, wind and currents, that results in a multi-directional load configuration (Fraunhofer IWES, 2009). Regardless, the geotechnical system considered in this paper has three degrees of freedom and the three loading components act in a single plane. Interestingly, Rudolph et al. (2014) investigated the cyclic behaviour of monopiles subjected to changing direction cyclic loading and found an amplification factor of 45% in 1*g* tests and 63% in centrifuge. In-plane loading conditions seem to have a beneficial effect on the accumulated displacements and therefore reduce the conservatism of the model.

In addition, the simplified method proposed does not account for the varying loading features of the cyclic load. However, this is important when real load time series are considered. In case a more sophisticated estimation of the accumulated displacements is needed, loading packages with different loading features could be included in the model, perhaps on the base of previous studies such as Peralta (2010) and LeBlanc et al. (2010b).

The empirical model is based on 1*g* tests only. Thus, it should be corroborated with centrifuge experiments or large-scale tests before using it with confidence in real design cases.

6. Conclusions

Bucket foundations have been extensively used and yet their behaviour under cyclic lateral loading is not fully explored. This paper presents a physical model and a comprehensive experimental campaign. The data analysis is focused on the long-term accumulated displacement and, particularly, on the rotational displacement. Some conclusions can be drawn about the general response of bucket foundations under cyclic loading.

The accumulation rate of the rotational displacement (calculated every ten cycles) is seen to reduce to negligible values within the first few hundreds of cycles, regardless of the load magnitude. The permanent displacement is not influenced by the loading frequency in the range tested (between 0.025 and 0.1 Hz). Post-cyclic curves are found different from the pure monotonic curves in terms of initial stiffness and ultimate capacity. This implies that, as expected, cyclic loading-induced permanent displacements affect the elasto-plastic proprieties of the geotechnical system.

The experimental data is also interpreted with an existing empirical model and new parameters are extrapolated. It is remarkably important to emphasise that the three bucket geometries tested seem to respond equally to cyclic loading. This means that, in the range of embedment ratio tested (0.5, 0.75 and 1) all the bucket geometries are equally influenced by cyclic loading. On the base of the empirical model, cyclic capacity curves are constructed and employed in a practical example.

Table 2. List of the experiments

Series 0	d/D	fL [Hz]	ζ_b	ζ_c
S30	1	-	-	-
S57	0.5	-	-	-
S48	0.75	-	-	-
Series 1				
C16	1	0.1	0.403	-0.047
C17	1	0.1	0.536	0.027
C18	1	0.1	0.304	-0.042
Series 2				
C20	1	0.1	0.358	-0.595
C22	1	0.1	0.383	0.193
C23	1	0.1	0.381	-0.426
C24	1	0.1	0.367	-0.963
C32	1	0.1	0.421	-0.146
C33	1	0.1	0.382	-0.316
C47	1	0.1	0.378	-0.796
Series 3				
C34	1	0.1	0.252	-0.604
C35	1	0.1	0.484	-0.543
C36	1	0.1	0.583	-0.563
C37	1	0.1	0.687	-0.578
C38	1	0.1	0.758	-0.583
C39	1	0.1	0.856	-0.588
C40	1	0.1	1.155	-0.469
Series 4				
C41	1	0.1	0.400	-0.514
C42	1	0.05	0.420	-0.500
C44	1	0.03	0.389	-0.598
C45	1	0.2	0.387	-0.479
C46	1	0.025	0.419	-0.500
Series 5				
C50	0.5	0.1	0.355	-0.054
C53	0.5	0.1	0.514	-0.049
C54	0.5	0.1	0.339	0.019
C55	0.5	0.1	0.398	0.040
Series 6				
C58	0.75	0.1	0.177	0.089
C59	0.75	0.1	0.244	0.055
C60	0.75	0.1	0.312	-0.055
C61	0.75	0.1	0.376	-0.053

References

Abadie CN and Byrne BW (2014) Cyclic loading response of monopile foundations in cohesionless soils. In *Proceedings of the 8th International Conference of Physical Modelling in Geotechnics (ICPMG)* (Gaudin C and White DJ (eds)). Taylor & Francis Group, London, UK, pp. 779-784.

Achmus M, Kuo Y-S and Abdel-Rahman K (2009) Behavior of monopile foundations under cyclic lateral load. *Computer and Geotechnics* **36(5)**: 725-735, http://dx.doi.org/10.1016/j.compgeo.2008.12.003

Achmus M, Thieken K, Akdag CT, Schröder C and Spohn C (2013a) Load bearing behaviour of bucket foundations in sand. In *Proceedings of the 3rd International Symposium on Computational Geomechanics (ComGeoIII)*, Krakow, Poland.

Achmus M, Akdag CT and Thieken K (2013b) Load-bearing behavior of suction bucket foundations in sand. Applied Ocean Research **43**: 157-165, http://dx.doi.org/10.1016/j.apor.2013.09.001

Andersen KH (2009) Bearing capacity under cyclic loading – offshore, along the coast, and on land. The 21st Bjerrum Lecture presented in Oslo, 23 November 2007. *Canadian Geotechnical Journal* **46(5)**: 513-535, http://dx.doi.org/10.1139/T09-003

Andersen KH, Puech AA and Jardine RJ (2013) Cyclic resistant geotechnical design and parameters selection for offshore engineering and other applications. In *Proceedings of TC 209 Workshop – Design for cyclic loading: piles and other foundations* (*ISSMGE)*, Paris, France, pp. 9-43.

Barari A and Ibsen LB (2012) Undrained response of bucket foundations to moment loading. *Applied ocean research* **36**: 12-21*,* http://dx.doi.org/10.1016/j.apor.2012.01.003

Butterfield R, Houlsby GT and Gottardi G (1997) Standardised sign conventions and notation for generally loaded foundations. *Géotechnique* **47(5)**: 1051-1054*,* http://dx.doi.org/10.1680/geot.1997.47.5.1051

Bye A, Erbrich C, Rognlien B and Tjelta TI (1995) Geotechnical design of bucket foundations. In *Proceedings of the Offshore Technology Conference (OTC)*, Houston, Texas, pp. 869-883.

Byrne BW (2010) *Investigations of suction caissons in dense sand*. Ph.D thesis, Oxford University, UK.

Cerato AB and Lutenegger AJ (2007) Scale effects of shallow foundation bearing capacity on granular material. *Journal of Geotechnical and Geoenvironmental Engineering* **133(10)**: 1192-1202, http://dx.doi.org/10.1061/(ASCE)1090-0241(2007)133:10(1192)

Depina I, Le TMH, Eiksund G and Benz T (2013) Cyclic behaviour of laterally loaded piles in soils with variable properties. In *Proceeding of the Twenty-third International Offshore and Polar Engineering (ISOPE)*, Anchorage, Alaska, USA, pp. 583-588.

DNV (Det Norske Veritas) (2011) DNV-OS-J101: Offshore standard: design of offshore wind turbine structures. DNV, Oslo, Norway.

Fraunhofer IWES (2010) Wind energy report Germany 2009 – Offshore. Fraunhofer IWES, Fassel, Germany.

Foglia A, Ibsen LB, Nielsen SK and Mikalauskas, L (2013). A preliminary study on bucket foundations under transient lateral loading. In *Proceeding of the Twenty-third International Offshore and Polar Engineering (ISOPE)*, Anchorage, Alaska, USA, pp. 465-471.

Garnier J (2013) Advances in lateral cyclic pile design: Contribution of the SOLCYP project. In *Proceedings of TC 209 Workshop – Design for cyclic loading: piles and other foundations (ISSMGE)*, Paris, France, pp. 59-68.

Gourvenec S (2007) Failure envelopes for offshore shallow foundations under general loading. *Géotechnique* **57(9)**: 715-728, http://dx.doi.org/10.1680/geot.2007.57.9.715

Ibsen LB, Barari A and Larsen KA (2014a) Adaptive plasticity model for bucket foundations. *ASCE Journal of Engineering Mechanics* **140(2)**: 361-373, http://dx.doi.org/10.1061/(ASCE)EM.1943-7889.0000633

Ibsen LB, Larsen KA and Barari A (2014b) Calibration of failure criteria for bucket foundations on drained sand under general loading. *Journal of Geotechnical and Geoenvironmental Engineering* **140(2)**, http://dx.doi.org/10.1061/(ASCE)GT.1943-5606.0000995

Jardine RJ, Andersen K and Puech A (2012) Cyclic loading of offshore piles: potential effects and practical design. Keynote Paper of the *7th International Conference on Offshore Site Investigations and Geotechnics*, Society for Underwater Technology, London, UK, pp. 59-100.

Kirkwood PB and Haigh SK (2014) Centrifuge testing of monopiles subject to cyclic lateral loading. In *Proceedings of the 8th International Conference of Physical Modelling in Geotechnics (ICPMG)* (Gaudin C and White DJ (eds)). Taylor & Francis Group, London, UK, pp. 827-831.

Klinkvort RT and Hededal O (2013). Lateral response of monopile supporting an offshore wind turbine. *Geotechnical Engineering* **166(2)**: 147-158, http://dx.doi.org/10.1680/geng.12.00033

LeBlanc C, Byrne BW and Houlsby GT (2010a). Response of stiff piles in sand to long-term cyclic lateral loading. *Géotechnique* **60(2)**: 79:90, http://dx.doi.org/10.1680/geot.7.00196

LeBlanc C, Byrne BW and Houlsby GT (2010b). Response of stiff piles to random two-way lateral loading. *Géotechnique* **60(9)**: 715:721, http://dx.doi.org/10.1680/geot.09.T.011

Peralta KP (2010) *Investigations on the behaviour of large diameter piles under long-term lateral cyclic loading in cohesionless soil*. Ph.D thesis, Leibniz University, Germany.

Randolph MF (2012) Offshore design approaches and model tests for sub-failure cyclic loading of foundations. In *Mechanical Behaviour of Soils under Environmentally-Induced Cyclic Loading* (di Prisco C and Wood DM (eds)). Springer, New York, USA.

Rudolph C, Grabe J and Bienen B (2014) Response of monopiles under cyclic lateral loading with a varying loading direction. In *Proceedings of the 8th International Conference of Physical Modelling in Geotechnics (ICPMG)* (Gaudin C and White DJ (eds)). Taylor & Francis Group, London, UK, pp. 453-458.

Senpere D and Auvergne A (1982) Suction anchor piles – a proven alternative to driving or drilling. In *Proceedings of the Offshore Technology Conference (OTC)*, Houston, Texas, pp. 483-493.

Taşan HE, Rackwitz F and Savidis S (2011) Experimentelle untersuchungen zum verhalten von zyklisch horizontal belasteten monopiles. Bautechnik **88(2)**: 102-112, http://dx.doi.org/ 10.1002/bate.201110010

Vesić, A.S. (1973). Analysis of ultimate loads of shallow foundations. *Journal of the Soil Mechanics and Foundations Division,* American Society of Civil Engineers 99(1): 45-73.

Villalobos FA (2006) *Model testing of foundations for offshore wind turbines*. Ph.D thesis, Oxford University, UK.

Villalobos FA, Byrne BW and Houlsby GT (2009) An experimental study of the drained capacity of suction caisson foundations under monotonic loading for offshore applications. *Soils and foundations* **49(3)**: 477-488.

Watson PG and Randolph MF (2009) A centriguge study into cyclic loading of caisson foundations. In *Proceedings of the 6th International Conference of Physical Modelling in Geotechnics (ICPMG)* (Ng CWW et al. (eds)). Taylor & Francis Group, London, UK, pp. 693-700, http://dx.doi.org/10.1201/NOE0415415866.ch99

Wood DM (2004) Geotechnical Modelling. CRC Press.

Zhu B, Byrne BW and Houlsby GT (2013) Long-term lateral cyclic response of suction caisson foundations in sand. Journal of Geotechnical and Geoenvironmental Engineering **139(1)**: 73-83, http://dx.doi.org/10.1061/(ASCE)GT.1943-5606.0000738

ISSN 1901-7278
DCE Technical Memorandum No. 49